Interference stabilization of Rydberg atoms enhanced by multiple V-type resonances

R. Parzyński and S. Wieczorek
Quantum Electronics Laboratory, Institute of Physics, A. Mickiewicz University, Umultowska 85, 61-614 Poznań, Poland
(Received 14 April 1998)

We introduce a model of laser pulse ionization of a high Rydberg state whose core is a chain of coupled V-type transitions with exact resonance in each arm of the V. Through this chain the population is allowed to migrate resonantly from the initial state of low angular momentum to other bound states of higher angular momenta, both of low and high energy. Along with the redistribution of the initial population over different bound states, we discuss the effect of the redistribution on atomic stabilization, exploiting an analytical solution of the model that holds in a limiting case. The resonant migration mentioned is shown to be able to enhance atomic stabilization against ionization by an optical-frequency pulse. [S1050-2947(98)02910-2]

PACS number(s): 32.80.Rm, 42.50.Hz

I. INTRODUCTION

One kind of atomic stabilization against ionization by a short laser pulse is known to be the stabilization of interference type [1]. It occurs when, in the manifold of a fixed-l state, the initially populated state becomes broadened by ionization to an extent comparable with its separation from the nearest initially empty neighbor. Under this condition, some population can be transferred from the initial state to the neighbor due to degenerate Raman transition. Then, destructive interference of the ionization paths from two (or more) populated states can result in a substantial suppression of ionization. The main concepts of interference stabilization were verified theoretically in numerical simulation as well as experimentally with the use of atoms prepared in high-Rydberg states [2].

In the standard theoretical approaches to interference stabilization, the models with two or several [3] and a large number of discrete states [4] of the same angular momentum were applied. More sophisticated models [5] allowed for the population to leave a fixed-l band of states and migrate to higher-angular-momentum Rydberg bands due to nonresonant degenerate Raman transitions. Also, models with a single fixed-l Rydberg band resonantly coupled by laser light to low-lying states were considered [6].

It is the aim of the present paper to describe a model of interference stabilization whose core is a number of V-type resonances linked in a chain. Each V-type resonance bridges two Rydberg bands of the angular momentum quantum numbers differing by 2. At the bottom of the V there is a low-lying resonant state of the angular momentum quantum number intermediate between the numbers of the Rydberg bands lying at the two tops of the V. As a matter of fact, we shall focus in the present paper on a specific limit of the model at which the solution to the population dynamics is reached analytically irrespective of how long the coupling chain is. We shall use the solution found to study the resonant migration of the population along the chain, i.e., to higher-l states placed both in the bottom and at the tops of the subsequent V. Finally, we will be able to conclude that this migration makes the Rydberg atom more resistant to ionization by an optical-frequency pulse.

II. THE MODEL AND ITS SOLUTION

Initially, the hydrogen atom is in the state $|0\rangle = |n_0 l_0 m_0 = l_0\rangle$, distinguished by the black dot in Fig. 1, which is a high Rydberg state ($n_0 \gg 1$) of a low angular momentum ($l_0 \ll n_0$). The initial state, along with other Rydberg states ($n \neq n_0$) of the same angular momentum as that of the initial one, forms a Rydberg band denoted by $j=0$ in Fig. 1. It is the lowest-angular-momentum Rydberg band of our model. The higher-angular-momentum Rydberg bands of the model are those denoted by $j=1,2,...,N$ in the figure and they have their angular momenta determined by l_0+2, l_0+4,..., l_0+2N, respectively. An optical frequency field of linear polarization along the z axis ($\Delta m=0$) couples perfectly resonantly the initial state to a lower lying state, $\lambda=1$ in the figure, of relatively low principal quantum number of the order of several units. Through the chain of resonant electric dipole couplings $\lambda=1 \rightarrow j=1 \rightarrow \lambda=2 \rightarrow j=2 \rightarrow \cdots \rightarrow \lambda=N \rightarrow j=N$, the population migrates then to both higher-angular-momentum Rydberg bands ($j=1-N$) and higher-angular-momentum λ states ($\lambda=2-N$), with all the latter ones of the principal quantum number the same as that of the $\lambda=1$ state. The length of the chain of couplings depends on the angular momentum of the initial state and the principal quantum number of the $\lambda=1$ state and, e.g., for

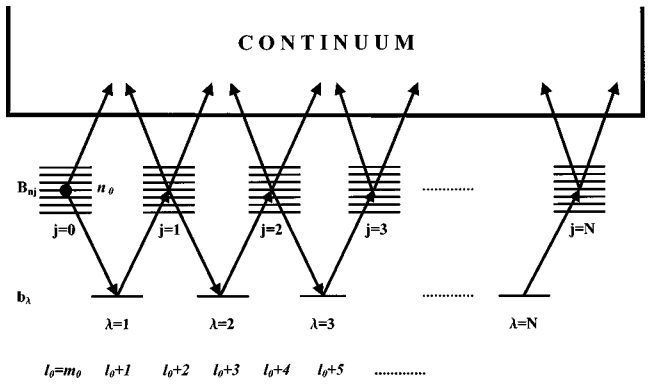

FIG. 1. Model of ionization from a high Rydberg state including a chain of V-type resonances through which the population migrates from the initial state to other bound states of higher angular momenta.

$l_0=0$ and $|\lambda=1\rangle=8p$ the length is determined by $N=4$. As seen, nonresonant migration of population between the neighboring Rydberg bands of our model was ignored as negligible when compared to resonant migration. We include, however, nonresonant Raman mixing via the continuum between different Rydberg states from a given angular momentum band.

Let $\Omega_{\lambda,nj}$ stand for the resonant Rabi frequency for the transition from the λ state to the nth Rydberg state in the jth band, and $D_{nj,n'j}$ for the nonresonant Raman coupling via the continuum between any two Rydberg states from the same band. The solution procedure, to be presented later on, is substantially simplified due to the fact that, for high principal quantum numbers, the above couplings are to a good approximation factorized [4,7] as $\Omega_{\lambda,nj}=f_n\Omega_{\lambda j}$ and $D_{nj,n'j}=f_nf_{n'}D_j$, where $f_n=n^{-3/2}$. We use this factorization ansatz throughout the paper as well as the rotating-wave and rectangular-pulse approximations. We also neglect the continuum-continuum transitions. Under these approximations, we write out standard differential equations for the Schrödinger population amplitudes of the λ states, b_λ, and the nth Rydberg states in all j bands, B_{nj}. Finally, we apply the Laplace transformation to these differential equations ($t\rightarrow s$, $b_\lambda\rightarrow\tilde{b}_\lambda$, $B_{nj}\rightarrow\tilde{B}_{nj}$), which results in the following set of coupled algebraic equations:

$$s\tilde{b}_\lambda+i\Omega_{\lambda,\lambda-1}K_{\lambda-1}+i\Omega_{\lambda,\lambda}K_\lambda=0, \tag{1}$$

$$\tilde{B}_{nj}=\frac{-f_n}{s-i\Delta_n}\,(i\Omega_{j,j}\tilde{b}_j+i\Omega_{j+1,j}\tilde{b}_{j+1}+D_jK_j)+\frac{\delta_{j0}\delta_{nn_0}}{s-i\Delta_n}, \tag{2}$$

where $K_j=\Sigma_n f_n\tilde{B}_{nj}$, $\delta_{\alpha\beta}$ is the Kronecker symbol showing where the population initially was, and Δ_n is the difference in frequency between the initially populated $|0\rangle$ state and any other Rydberg state. When writing these equations we used the condition of the exact resonance between the initially populated $|0\rangle$ and the $\lambda=1$ states as well as the fact that Δ_n was independent of j due to the orbital degeneracy of the hydrogenic levels.

Multiplying Eq. (2) by f_n and then summing it over all n in a given Rydberg band we obtain the alternative expression for $\tilde{B}_{nj}$:

$$\tilde{B}_{nj}=\frac{f_n}{s-i\Delta_n}\,\frac{1}{P}\left(K_j-\frac{f_{n_0}}{s}\,\delta_{j0}\right)+\frac{\delta_{j0}\delta_{nn_0}}{s-i\Delta_n}, \tag{3}$$

where

$$K_j=-iPG_j(\Omega_{j,j}\tilde{b}_j+\Omega_{j+1,j}\tilde{b}_{j+1})+\frac{f_{n_0}}{s}\,G_j\delta_{j0}, \tag{4}$$

$$P=\sum_n\,\frac{f_n^2}{s-i\Delta_n}, \tag{5}$$

$$G_j=\frac{1}{1+PD_j}. \tag{6}$$

By the use of the above K_j we convert Eq. (1) into the matrix-form equation for $\tilde{b}_\lambda$ alone:

$$M\begin{bmatrix}\tilde{b}_1\\ \tilde{b}_2\\ \vdots\\ \tilde{b}_N\end{bmatrix}=\begin{bmatrix}-i\Omega_{1,0}f_{n_0}G_0/s\\ 0\\ \vdots\\ 0\end{bmatrix}, \tag{7}$$

where M is the tridiagonal symmetric matrix

$$M=\begin{bmatrix}A_1 & B_1 & 0 & 0 & 0 & \cdots & & 0\\ B_1 & A_2 & B_2 & 0 & 0 & & & \\ 0 & B_2 & A_3 & B_3 & 0 & & & \\ \vdots & & & & \ddots & & & \\ & & & & & & & \\ & & & & & B_{N-2} & A_{N-1}B_{N-1} & \\ 0 & & & & & & B_{N-1}A_N & \end{bmatrix} \tag{8}$$

with the elements

$$A_\alpha=s+PG_{\alpha-1}\Omega_{\alpha,\alpha-1}^2+PG_\alpha\Omega_{\alpha,\alpha}^2, \tag{9}$$

$$B_\alpha=PG_\alpha\Omega_{\alpha,\alpha}\Omega_{\alpha+1,\alpha}, \tag{10}$$

where α runs 1,2,...,N. To remind, the left index in $\Omega_{a,b}$ refers to the λ state while the right one to the j band in our model from Fig. 1.

There is one case, at least, that allows a compact analytical solution to Eq. (7) and then a relatively simple analytical transformation of this Laplace solution to the time domain ($\tilde{b}_\lambda\rightarrow b_\lambda$) irrespective of how large N is. The case we focus hereafter on is determined by l-independent couplings ($\Omega_{\lambda,j}=\Omega$, $D_j=D$) and results in $A_1=A_2=\cdots=A_N=A=s+2PG\Omega^2=s+2B$ and $B_1=B_2=\cdots=B_N=B=PG\Omega^2$, where $G=G_1=G_2=\cdots=G_N$. Though departing from what we meet in the real hydrogen atom, the approximation of l-independent couplings is sometimes applied [8] to achieve qualitative insight into the population dynamics of a multistate atom in an intense optical-frequency field. In this approximation, which, in fact, overestimates the couplings for large-l numbers, the close-form solution to Eq. (7) is a far fetched generalization of the formula of Grobe *et al.* [8] and reads

$$\tilde{b}_\lambda=i(-1)^\lambda\,\frac{f_{n_0}}{\Omega}\,\frac{1}{sP}\,F_\lambda, \tag{11}$$

where

$$F_\lambda=\frac{\sin[(N+1-\lambda)\phi]}{\sin[(N+1)\phi]} \tag{12}$$

and

$$\phi=\arccos\left(\frac{A}{2B}\right). \tag{13}$$

F_λ has its poles determined by the equation

$$\frac{A}{2B}=\cos\left(\frac{k\pi}{N+1}\right),\quad k=1,...,N, \tag{14}$$

which, for a given k, has to be solved with respect to the Laplace variable, leading to p solutions $s_{p,k}$. The residuum $R^{\lambda}_{p,k}$ of F_{λ} at $s_{p,k}$ is then found as $R^{\lambda}_{p,k}=\Omega^2 C^{\lambda}_{p,k}$, where

$$C^{\lambda}_{p,k}=C^{\lambda}_{k}\left(\frac{PG}{1-s\,\dfrac{G}{P}\,\dfrac{dP}{ds}}\right)_{s=s_{p,k}} \tag{15}$$

with

$$C^{\lambda}_{k}=(-1)^{k+1}\,\frac{2}{N+1}\,\sin\left(\frac{k\pi}{N+1}\right)\sin\left(\frac{N+1-\lambda}{N+1}\,k\pi\right). \tag{16}$$

All this enables us to decompose F_{λ} into the elementary fractions

$$F_{\lambda}=\Omega^2\sum_{p,k}\ \frac{C^{\lambda}_{p,k}}{s-s_{p,k}}. \tag{17}$$

Similarly, we decompose $1/(sP)$, namely,

$$\frac{1}{sP}=\frac{\prod_{n\neq n_0}(s-i\Delta_n)}{\sum_{n'} f^2_{n'}\prod_{n\neq n'}(s-i\Delta_n)}=\frac{f(s)}{g(s)}$$
$$=\alpha+\frac{h(s)}{g(s)}=\alpha+\sum_{q}\ \frac{R_q}{s-s_q}, \tag{18}$$

where α and $h(s)$ are found when dividing the two polynomials $f(s)$ and $g(s)$ of the same order, s_q are the poles of the rational function $h(s)/g(s)$, and R_q is the residuum of this function at a given s_q. As a result, Eq. (11) for $\tilde{b}_{\lambda}$ is replaced by

$$\tilde{b}_{\lambda}=i(-1)^{\lambda}f_{n_0}\Omega\sum_{p}\ \sum_{k=1}^{N}\left(\alpha+\sum_{q}\ \frac{R_q}{s-s_q}\right)\frac{C^{\lambda}_{p,k}}{s-s_{p,k}}. \tag{19}$$

By the use of the convolution theorem, the above $\tilde{b}_{\lambda}$ is straightforwardly transformed into the time-dependent Schrödinger population amplitude b_{λ}:

$$b_{\lambda}=i(-1)^{\lambda}f_{n_0}\Omega\sum_{p}\ \sum_{k=1}^{N}\left[\alpha+\sum_{q}\ R_q f(s_q-s_{p,k},t)\right]$$
$$\times C^{\lambda}_{p,k}e^{s_{p,k}t}, \tag{20}$$

where

$$f(x,t)=\frac{e^{xt}-1}{x}. \tag{21}$$

Now, we go back to Eq. (3) and Eq. (4) in order to find $\tilde{B}_{nj}$ and then B_{nj} in closed forms under the approximation of l-independent couplings. In this context, the first thing we wish to stress is that $\tilde{B}_{nj}$ includes as its part the term $G/(s-i\Delta_n)$, which is convenient to decompose into the elementary fractions:

$$\frac{G}{s-i\Delta_n}=\frac{\prod_{n'\neq n}(s-i\Delta_{n'})}{\prod_{n'}(s-i\Delta_{n'})+D\sum_{n''}f^2_{n''}\prod_{n'\neq n''}(s-i\Delta_{n'})}$$
$$=\sum_{r}\ \frac{R_r}{s-s_r}, \tag{22}$$

where s_r are the roots of the denominator. The other thing is that $\Omega_{0,0}=0$, if $j=0$, as well as $\Omega_{N+1,N}=0$, if $j=N$. With these points and Eq. (19) for $\tilde{b}_{\lambda}$ taken into account, one obtains (i) for $j=0$,

$$\tilde{B}_{n0}=-if_n\Omega\tilde{T}_{n1}-\frac{f_{n_0}f_nD}{s}\sum_{r}\ \frac{R_r}{s-s_r}+\frac{\delta_{nn_0}}{s}; \tag{23}$$

(ii) for $j=N$,

$$\tilde{B}_{nN}=i(-1)^{N}f_n\Omega\tilde{T}_{nN}; \tag{24}$$

(iii) for $j=1,2,\ldots,N-1$,

$$\tilde{B}_{nj}=i(-1)^{j}f_n\Omega(\tilde{T}_{nj}-\tilde{T}_{n\,j+1}); \tag{25}$$

where

$$\tilde{T}_{n\lambda}=(-1)^{\lambda+1}\tilde{b}_{\lambda}\sum_{r}\ \frac{R_r}{s-s_r}$$
$$=-if_{n_0}\Omega\sum_{r}\ \frac{R_r}{s-s_r}\sum_{p}\ \sum_{k=1}^{N}\left(\alpha+\sum_{q}\ \frac{R_q}{s-s_q}\right)\frac{C^{\lambda}_{p,k}}{s-s_{p,k}}. \tag{26}$$

The convolution theorem, when applied to the above equations, results then in the following time-dependent Schrödinger population amplitudes B_{nj}: (i) for $j=0$,

$$B_{n0}=-if_n\Omega T_{n1}-f_{n_0}f_nD\sum_{r}\ R_r f(s_r,t)+\delta_{nn_0}; \tag{27}$$

(ii) for $j=N$,

$$B_{nN}=i(-1)^{N}f_n\Omega T_{nN}; \tag{28}$$

(iii) for $j=1,2,\ldots,N-1$,

$$B_{nj}=i(-1)^{j}f_n\Omega(T_{nj}-T_{n\,j+1}); \tag{29}$$

with

$$T_{n\lambda}=-if_{n_0}\Omega\sum_{r}\ R_r e^{s_r t}\sum_{p}\ \sum_{k=1}^{N}\left[\alpha f(s_{p,k}-s_r,t)\right.$$
$$\left.+\sum_{q}\ \frac{R_q}{s_q-s_{p,k}}\left[f(s_q-s_r,t)-f(s_{p,k}-s_r,t)\right]\right]C^{\lambda}_{p,k}, \tag{30}$$

and the function $f(x,t)$ defined by Eq. (21).

III. ILLUSTRATIVE RESULTS

The advantage of Eq. (20) for b_λ and Eqs. (27)–(30) for B_{nj} is that with them the problem of the population dynamics has been reduced to finding the poles $s_{p,k}$ from Eq. (14), s_q from Eq. (18), and s_r from Eq. (22). Below, we shall consider two illustrative cases that allow these poles to be found analytically. One case is when we leave only one state in each Rydberg band ($n=n_0$), and the other when each Rydberg band is approximated by a flat, infinite, equidistant Bixon-Joertner structure [9].

For the model with the single state in each Rydberg band, $P=f_{n_0}^2/s$. This leads to

$$s_{p,k}=\tfrac{1}{2}[-D_{n_0}+(-1)^p x_k], \quad p=1,2,$$

$$x_k=\sqrt{D_{n_0}^2-8\beta_k\Omega_{n_0}^2}, \quad \beta_k=1-\cos\left(\frac{k\pi}{N+1}\right), \tag{31}$$

$$D_{n_0}=f_{n_0}^2 D, \quad \Omega_{n_0}=f_{n_0}\Omega,$$

and $\alpha=f_{n_0}^{-2}$, $R_q=0$ as well as $s_r=s_1=-D_{n_0}$, $R_r=R_1=1$, resulting in

$$b_\lambda=i(-1)^\lambda 2\Omega_{n_0}e^{-D_{n_0}t/2}\sum_{k=1}^{N}\frac{C_k^\lambda}{x_k}\sinh(x_kt/2) \tag{32}$$

and

$$T_{n_0\lambda}=\frac{-i}{2\Omega_{n_0}}e^{-D_{n_0}t/2}\sum_{k=1}^{N}\frac{C_k^\lambda}{\beta_k}\left(\frac{D_{n_0}}{x_k}\sinh(x_kt/2)-\cosh(x_kt/2)+e^{-D_{n_0}t/2}\right). \tag{33}$$

For the model with the Bixon-Joertner structure in the place of Rydberg bands, $P=f_{n_0}^2(\pi/\Delta)\coth(\pi s/\Delta)$, where Δ means the level spacing in the units of frequency. Assuming the laser pulse to be shorter than the specific Kepler period for the Bixon-Joertner structure, $\tau=2\pi/\Delta$, the above P is reduced to $P=f_{n_0}^2(\pi/\Delta)$ [9], and we interpret Δ as the distance between the Rydberg level with $n=n_0$ and its nearest neighbor. In this case

$$s_{p,k}=s_k=-2\pi\Delta\beta_k(\Omega_{n_0}/\Delta)^2u, \qquad u=\frac{1}{1+(\pi D_{n_0}/\Delta)}, \tag{34}$$

$\alpha=0$, $s_q=s_1=0$, $R_q=R_1=\Delta/(\pi f_{n_0}^2)$ and $s_r=s_1=i\Delta_n=i(n_0-n)\Delta$, $R_r=R_1=u$, leading to

$$b_\lambda=i(-1)^\lambda\Omega_{n_0}u\sum_{k=1}^{N}C_k^\lambda f(s_k,t) \tag{35}$$

and

$$T_{n\lambda}=-i\Omega_{n_0}e^{i\Delta_n t}u^2\sum_{k=1}^{N}\frac{C_k^\lambda}{s_k}[f(s_k-i\Delta_n,t)-f(-i\Delta_n,t)]. \tag{36}$$

Then, we insert $T_{n\lambda}$ of Eq. (36) into Eqs. (27)–(29) for the amplitudes B_{nj}, take the square modulus of these amplitudes, and finally sum the results over n exploiting the summation relation

$$\sum_{n=-\infty}^{\infty}f(s_k-in\Delta,t)f^*(s_l-in\Delta,t)=\frac{2\pi}{\Delta}f(s_k+s_l^*,t). \tag{37}$$

As a result, we arrive at the following fractions $W_j=\Sigma_n|B_{nj}|^2$ of the population left in the subsequent Bixon-Joertner bands at the end of the pulse of duration $t/\tau\leqslant 1$: (i) for $j=0$,

$$\begin{aligned}W_0=1&+(2\pi)^2|uD_{n_0}/\Delta|^2\frac{t}{\tau}-4\pi\,\mathrm{Re}(uD_{n_0}/\Delta)\frac{t}{\tau}\\&+(2\pi)^4(\Omega_{n_0}/\Delta)^4|u|^4\sum_{k,l=1}^{N}\frac{C_k^1C_l^1}{z_kz_l^*}\left[f\left(z_k+z_l^*,\frac{t}{\tau}\right)-f\left(z_k,\frac{t}{\tau}\right)-f\left(z_l^*,\frac{t}{\tau}\right)+\frac{t}{\tau}\right]\\&+2(2\pi)^2(\Omega_{n_0}/\Delta)^2\sum_{k=1}^{N}C_k^1\,\mathrm{Re}\left\{\frac{u^2}{z_k}\left[f\left(z_k,\frac{t}{\tau}\right)-\frac{t}{\tau}\right]\times[2\pi(uD_{n_0}/\Delta)^*-1]\right\};\end{aligned} \tag{38}$$

(ii) for $j=N$,

$$W_N=(2\pi)^4(\Omega_{n_0}/\Delta)^4|u|^4\sum_{k,l=1}^{N}\frac{C_k^NC_l^N}{z_kz_l^*}\left[f\left(z_k+z_l^*,\frac{t}{\tau}\right)-f\left(z_k,\frac{t}{\tau}\right)-f\left(z_l^*,\frac{t}{\tau}\right)+\frac{t}{\tau}\right]; \tag{39}$$

(iii) for $j=1,2,...,N-1$,

$$W_j=(2\pi)^4(\Omega_{n_0}/\Delta)^4|u|^4\sum_{k,l=1}^{N}\frac{(C_k^j-C_k^{j+1})(C_l^j-C_l^{j+1})}{z_kz_l^*}\times\left[f\left(z_k+z_l^*,\frac{t}{\tau}\right)-f\left(z_k,\frac{t}{\tau}\right)-f\left(z_l^*,\frac{t}{\tau}\right)+\frac{t}{\tau}\right]; \tag{40}$$

where $z_k=2\pi s_k/\Delta$.

Figures 2 and 3 are graphical presentations of the results obtained with the use of the close-form equations (32) and (33) as well as (38)–(40). These figures were obtained assuming the length of the coupling chain to be determined by $N=4$ and they show the population versus laser intensity in the j-Rydberg bands (a), λ states (b), and atomic continuum (c). The assumed length of the chain is specific for the case when, e.g., the initially populated Rydberg state $n_0s=40s$ is resonantly coupled to the $|\lambda=1\rangle=8p$ state. As the representative atomic parameters we took $\Omega_n=10^7I^{1/2}$ and D_n

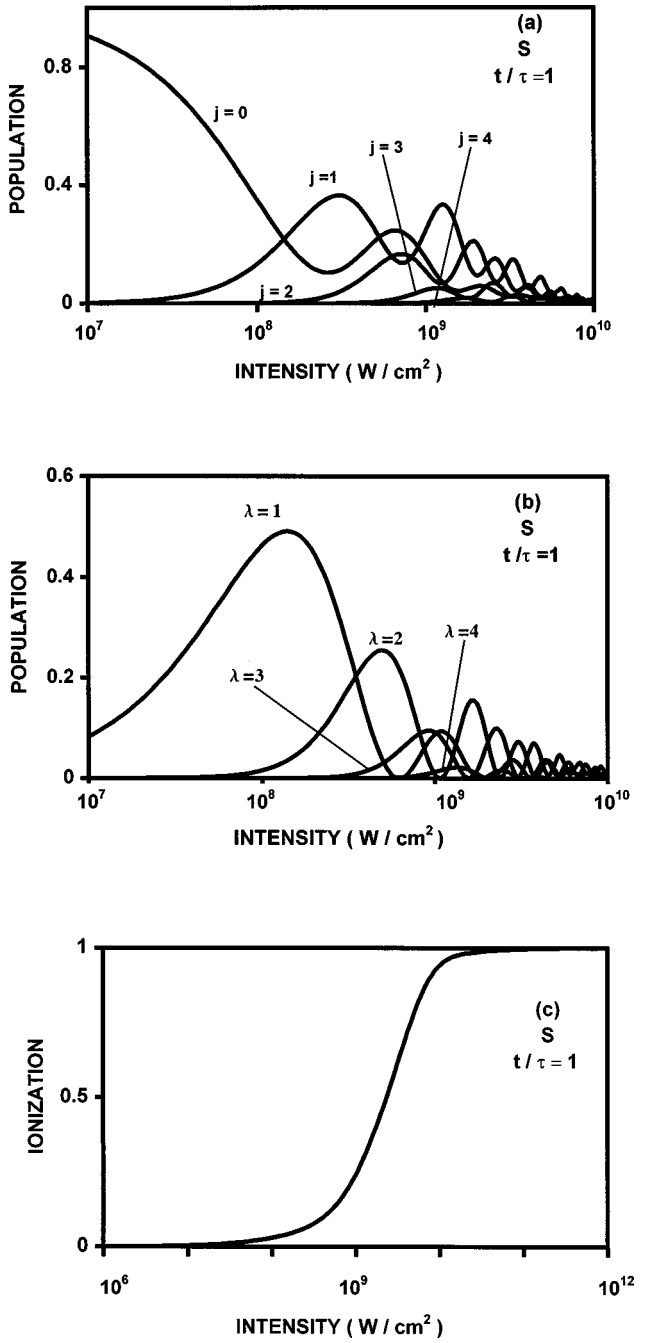

FIG. 2. Population vs laser intensity in the j-Rydberg bands (a), low-lying resonant λ states (b), and atomic continuum (c), for the model with a sequence of $N=4$ V-type resonances and only one state included in each Rydberg band (S). The pulse duration equals to the Kepler period of the $n_0=40$ Rydberg state.

$=20(1+i20)I$, where I is laser intensity in W/cm^2. The above Ω_n is approximately (i.e., with the factor of 1.19 dropped) the resonant Rabi frequency for the $40s\rightarrow 8p$ transition, Re(D_n) is nearly (i.e., with the factor of 0.75 dropped) half of the ionization rate of the 40s state, while Im(D_n) is taken in analogy to the paper of Grobe *et al.* [8]. Both Ω_n and Re(D_n) were calculated by us exactly using the Laplace-transform approach of Feldman, Fulton, and Judd [10], and the values found in this way were checked to be close to those resulting from the quasiclassical approach of Adams, Fedorov, and Meyerhofer [7]. Figure 2 refers to the model

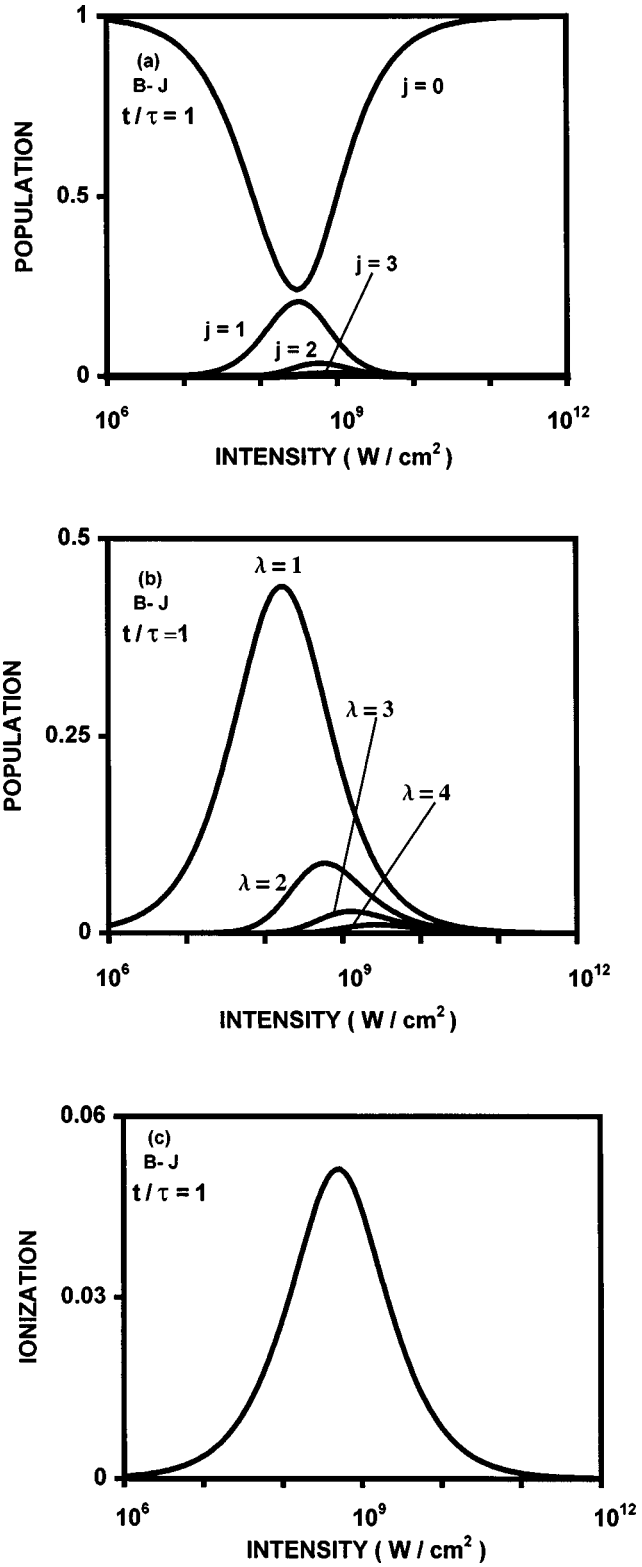

FIG. 3. Same as in Fig. 2 except for the model with Rydberg bands approximated by the Bixon-Joertner structures (B-J).

with only a single Rydberg state ($n=n_0=40$) taken into account in each Rydberg band (S), while Fig. 3—to the model with each Rydberg band approximated by the Bixon-Joertner structure (B-J). Both figures were made assuming the pulse duration to be equal to the Kepler period of the $n_0=40$ Rydberg state ($t=\tau=2\pi/\Delta=9.7$ ps). For other pulse durations, shorter than the Kepler period, we observed only quan-

titative differences as compared to Figs. 2 and 3, without any qualitatively new kinds of behavior.

Figures 2 and 3 point to a potentially possible resonant migration of the population along the coupling chain, i.e., from the initially populated high-Rydberg state of low angular momentum to both the j-Rydberg bands and λ states of higher angular momenta ($j=1-4$; $\lambda=2-4$). Strikingly, the migration appears to be efficient at intensities intermediate between low and high ones and it stops in the limit of high intensities. This conclusion emerges from both models, i.e., the S model with a single state left in each Rydberg band and the (B-J) model with the Bixon-Joertner structure of the bands. There is, however, a fundamental difference between the predictions of the two models. In the S model, no population is left in any discrete state at the end of the pulse if intensity is high and, as a result, the ionization is complete in this intensity limit [see, Fig. 2(c)]. By contrast, the (B-J) model predicts that, at high intensities, all the population is kept in the lowest-angular-momentum Rydberg band [$j=0$ in Fig. 3(a)], i.e., the band including the initially populated state. This gives rise to the high-intensity stabilization as shown in Fig. 3(c). Figure 3(c), when compared with Fig. 2(c), presents the dramatic effect of the number of states in consecutive Rydberg bands and, thus, the interference between different ionization paths on ionization/stabilization. Let us note that the threshold of stabilization observed ($\sim 10^9$ W/cm^2) nearly satisfies the condition $\Omega_n \simeq \Delta$ rather than $\mathrm{Re}(D_n) \simeq \Delta$, where $\Delta = 6.5\times 10^{11}$ s^{-1}. It would correspond to what Fedorov and Poluektov [6] call the V-type interference stabilization.

Figure 4(a) corresponds to the (B-J) model, and it shows a comparison of the ionization curve from Fig. 3(c) ($N=4$) with the corresponding curves obtained by having restricted ($N=1$) or completely neglected ($N=0$) the resonant migration of the population from the lowest-angular-momentum Rydberg band to bound states of higher angular momenta. The curve for $N=1$ was prepared allowing the population to migrate to the $\lambda=1$ state and $j=1$ band only, while the curve for $N=0$ with ignoring the coupling of the $j=0$ band to the $\lambda=1$ state at all. The main effect of restriction/neglect of the population migration is manifested in the height of the curve of ionization versus laser intensity—with the migration restricted/neglected the curve rises, i.e., the ionization increases. Thus, as results from Fig. 4(a), the interference stabilization is enhanced upon the resonant V-type migration of the population towards bound states of the angular momenta higher than that of the initial state.

We have verified this general conclusion by changing arbitrarily the imaginary part in the nonresonant-Raman coupling parameter D_n. The conclusion remained unchanged but we made two additional observations. The one is that the height of the curves from Fig. 4(a) increases when diminishing the imaginary part in D_n. The curves were found to be the highest when $\mathrm{Im}(D_n)=0$. This case is shown in Fig. 4(b). The other observation, evident from Fig. 4(b), concerns the shift of the threshold of stabilization towards higher intensities when diminishing $\mathrm{Im}(D_n)$. In the case of Fig. 4(b), the stabilization begins at the intensity of 10^{10} W/cm^2, close to that resulting from the condition $\mathrm{Re}(D_n) \simeq \Delta$ rather than $\Omega_n \simeq \Delta$. In the language of the paper of Fedorov and Poluektov [6] this higher threshold intensity could be the manifestation of the Λ-type interference stabilization.

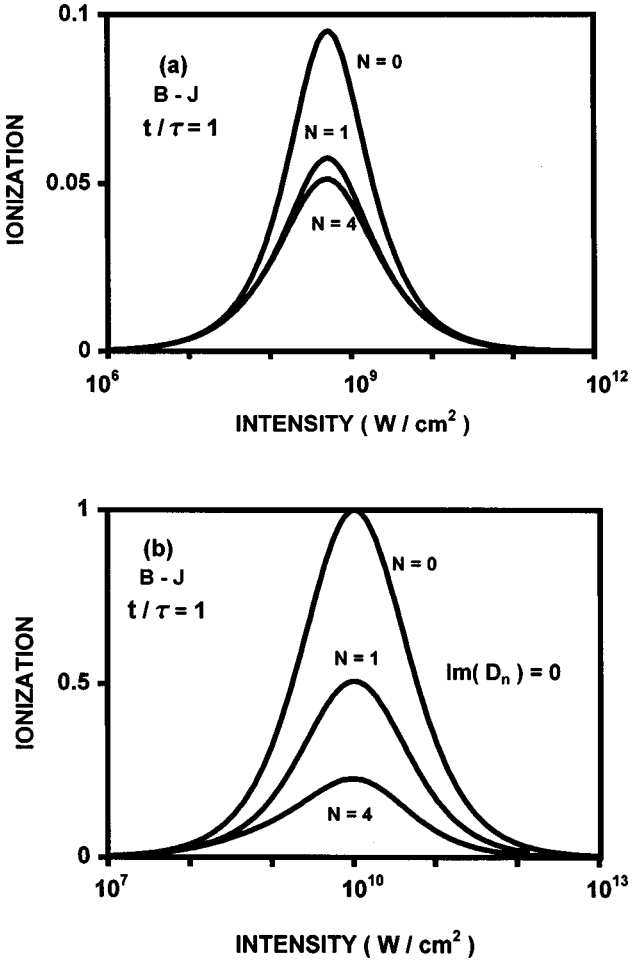

FIG. 4. Ionization vs laser intensity for the (B-J) model and different number N of V-type resonances in the migration chain ($N=4,1,0$).

IV. CONCLUSIONS

The general conclusion emerging from our analysis is that, when an atom prepared in a high Rydberg state of low angular momentum is one-photon ionized by an optical-frequency pulse, then the resonant migration of population towards bound states of higher angular momenta through the chain of V-type transitions makes the atom more resistant to ionization. This conclusion, derived from our analytical solution restricted to pulses not longer than one Kepler period of the initial high-Rydberg state, is planned to be verified in future in the long-pulse scale. In this scale and with many states included in the subsequent Rydberg bands of different angular momenta, substantial numerical effort is expected to be unavoidable, as distinct from the present paper.

ACKNOWLEDGMENT

One of us (R.P.) gratefully acknowledges support from the Polish Committee for Scientific Research under Grant No. 2 PO3B 078 12.

[1] H. G. Muller, in *Super-Intense Laser-Atom Physics IV*, edited by H. G. Muller and M. V. Fedorov (Kluwer Academic, Dordrecht, 1996), p. 1.

[2] M. Gajda, B. Piraux, and K. Rzążewski, Phys. Rev. A **50**, 2528 (1994); R. R. Jones and P. H. Bucksbaum, Phys. Rev. Lett. **67**, 3215 (1991); L. D. Noordam, H. Stapelfeldt, D. I. Duncan, and T. F. Gallagher, *ibid.* **68**, 1496 (1992); J. H. Hoogenraad, R. B. Vrijen, and L. D. Noordam, Phys. Rev. A **50**, 4133 (1994); N. E. Tielking and R. R. Jones, *ibid.* **52**, 1371 (1995).

[3] J. Parker and C. R. Stroud, Jr., Phys. Rev. A **41**, 1602 (1990); L. Roso-Franco, G. Orriols, and J. H. Eberly, Laser Phys. **2**, 741 (1992).

[4] M. V. Fedorov, Laser Phys. **3**, 219 (1993); M. V. Fedorov, M. Yu. Ivanov, and A. M. Movsesyan, J. Phys. B **23**, 2245S (1990); M. V. Fedorov and A. M. Movsesyan, J. Opt. Soc. Am. B **6**, 928 (1989); A. Wójcik and R. Parzyński, Phys. Rev. A **50**, 2475 (1995).

[5] K. Im, R. Grobe, and J. H. Eberly, Phys. Rev. A **49**, 2853 (1994); M. V. Fedorov, M. M. Tehranchi, and S. M. Fedorov, J. Phys. B **29**, 2907 (1996); R. Parzyński and A. Wójcik, Laser Phys. **7**, 551 (1997).

[6] A. Wójcik and R. Parzyński, Phys. Rev. A **50**, 2475 (1995); J. Opt. Soc. Am. B **12**, 369 (1995); M. V. Fedorov and N. B. Poluektov, Laser Phys. **7**, 299 (1997).

[7] M. S. Adams, M. V. Fedorov, and D. D. Meyerhofer, Phys. Rev. A **52**, 125 (1995).

[8] Z. Białynicka-Birula, I. Białynicki-Birula, J. H. Eberly, and B. W. Shore, Phys. Rev. A **16**, 2048 (1977); R. Grobe, G. Leuchs, and K. Rzążewski, *ibid.* **34**, 1188 (1986); R. Parzyński and A. Grudka, *ibid.* **58**, 1335 (1998).

[9] G. C. Stey and W. Gibberd, Physica (Amsterdam) **60**, 1 (1972).

[10] G. Feldman, T. Fulton, and B. R. Judd, Phys. Rev. A **51**, 2762 (1995).